Flight Characteristics of AAM/UAM-Scale Quadcopters Under Atmospheric Turbulence

Matthew Bahr
bahrm2@rpi.edu
Graduate Research Assistant

Etana Ferede
ferede@rpi.edu
Lecturer

Farhan Gandhi
gandhf@rpi.edu
Redfern Professor and MOVE Director

Center for Mobility with Vertical Lift (MOVE)
Rensselaer Polytechnic Institute
Troy, NY, United States

ABSTRACT

The flight responses of quadcopters of various scales (50-1200 lb) are evaluated in the presence of a 20 kt turbulent headwind. Nominal flight controllers are tuned for each aircraft to meet HQ specifications, where the controllers will reject disturbances to the aircraft groundspeed, attempting to maintain zero groundspeed. Froude-scaling is performed to scale the handling qualities specifications of the smaller aircraft, utilizing the additional agility. The nominal and scaled controllers are then compared in rejecting disturbance due to the turbulent headwind. Non-linear dynamic simulations are performed to evaluate the rigid body response of each aircraft, finding that scaling the flight controllers (on aircraft less than 1200 lb) reduces the pitch and roll attitude response so that all aicraft have similar peak-to-peak values. Following scaling, the peak-to-peak roll and pitch attitudes for all four aircraft are within 0.5° and 0.4° of each other, respectively. The improvement in disturbance rejection capabilities from scaling comes at the cost of 24% increase in the RMS current, and 2% additional current margin for the 50 lb aircraft (which is the largest increase). Overall, the increase in actuator activity due to scaling the controllers is less than the current margin required for maneuvering, resulting in the motors not needing to increase in size.

INTRODUCTION

In recent years, the operation of aircraft in urban environments has moved significantly closer to being a reality, driven by advances in technology associated with eVTOL aircraft and the collective effort of government, academia, and the private sector. The vehicles operating within the scope of Advanced Air Mobility (AAM) will be required to safely complete various missions in many challenging environments, while sharing crowded airspace in the presence of both pedestrians and infrastructure. A critical element of successful operation within urban environments is the performance of eVTOL aircraft in the presence of atmospheric turbulence.

In the past, there has been extensive effort in evaluating the performance of conventional helicopters in turbulent conditions; one such example is rotorcraft operation within ship airwakes. A recent study by Thedin et al. (Ref. 1) compared two methods of modeling the atmospheric boundary layer and simulated the effects on a rotorcraft at multiple stations within the ship wake. A significant finding of this study was that the command inputs to maintain the desired station occur at low frequency (0.1-3 Hz range), which compared well with flight test data. Another study by Oruc et al. (Ref. 2) evaluated the coupling of rotorcraft dynamic simulations and CFD simulations for aircraft operating in ship airwakes. The authors found that fully coupled simulations predict higher frequency and amplitude perturbations compared to the one-way coupling (effcts of ship airwake only); however, these flight simulations came at a significant computational cost (similar to CFD simulation cost).

While significant work has been done to model atmospheric turbulence on conventional rotorcraft, the aircraft that will occupy the AAM market will feature novel designs. Therefore, it is crucial to evaluate these new configurations thoroughly. One such configuration is a quadcopter concept, introduced by the Revolutionary Vertical Lift Technology (RVLT) project, which has been modeled as a single to six passenger aircraft (1200-6500 lb gross weight) (Ref. 3). Other studies from NASA have focused on the design of flight controllers for the variable pitch or variable rotor speed controlled quadcopters, where Malpica and Withrow-Maser (Refs. 4,5) found that meeting Level 1 handling qualities can be difficult when using variable-RPM rotor control.

At RPI, recent studies have also focused on the handling qualities of multicopters sized for AAM operations. Walter et al. (Ref. 6) applied scaled (based on rotor size) handling qualities requirements to quadcopters ranging in size from 300 lb to 1200 lb and evaluated the performance and actuator requirements when executing various maneuvers and rejecting discrete gusts. In a similar study, Bahr et al. (Ref. 7) applied standard HQ specifications to a quadcopter, hexacopter, and

Presented at the Vertical Flight Society's 78th Annual Forum & Technology Display, Ft. Worth, Texas, USA, May 10–12, 2022.

octocopter (all 1200 lb) and also examined various maneuvers and discrete gusts. Both of these studies found that the actuator effort required to execute maneuvers exceeded what was required to reject discrete gusts. Most recently, atmospheric turbulence was applied to the 1200 lb quadcopter (modeled in Refs. 6 and 7) where a precursor CFD simulation was used to generate a turbulent flow field that was applied to the aircraft in a flight dynamics simulation (Ref. 8). The study found that the flight controllers tuned to standard HQ specifications did well in rejecting the applied turbulence, where the turbulent wind content (and actuator effort to reject the turbulence) was in the 0.1-3 Hz frequency range.

The present study applies atmospheric turbulence to quadrotor eVTOL aircraft of various scales to explore how the different vehicles respond to disturbance caused by turbulence. The response of each aircraft will be examined in the context of peak-to-peak rigid body response as well as the actuator effort required to reject the turbulence. Further, flight controllers for the smaller aircraft (<1200 lb) will be scaled to improve the disturbance rejection capabilities. The performance of the scaled controllers will be compared to the nominal controllers using the same metrics, overall evaluating the cost associated with improved performance.

MODELING

The aircraft modeled in this study feature fixed-pitch, variable-RPM rotors and utilize the Rensselaer Multicopter Analysis Code (RMAC, Ref. 9); RMAC is a physics-based code which calculates rotor forces and moments using blade element theory and a 10-state Peters-He dynamic inflow model (Ref. 10). RMAC is used to linearize the model (about hover) for flight control design. When the vehicles are simulated in the presence of turbulence the full non-linear dynamics are evaluated within RMAC and the time history response is computed using a stiff, variable-step solver within Simulink®.

Quadcopters at four scales are evaluated in the presence of turbulence, where the parameters common to all scales are tabulated in Table 1 and the varying parameters are shown in Table 2. The rotor booms are sized to maintain at 10% rotor radius tip clearance and the vehicle inertia is scaled from the 1200 lb aircraft (where inertia scales with weight$^{5/3}$, Ref. 11).

Table 1. Common Aircraft Parameters

Parameter	
Number of Rotors	4
Disk Loading	6 lb/ft^2
Tip Clearance	$0.1R$
Solidity	0.0646
Blade Root Pitch	21.52°
Blade Twist	−10.39°

Table 2. Aircraft Parameters

Gross Weight (lb)	50	300	680	1200
Rotor Radius (ft)	0.81	2	3	4
Boom Length (ft)	1.20	2.97	4.45	5.94
I_{xx} (slug ft^2)	1.3	32	128	344
I_{yy} (slug ft^2)	1.6	38	150	405
I_{zz} (slug ft^2)	2.5	62	246	668

Turbulence

The turbulent flow field used in this study is the same flow field discussed in Ref. 8, where a resolved, turbulent field is generated and convected downstream over the aircraft. TurbSim (developed by NREL, Ref. 12) is used to generate the resolved turbulent flow field; and PHASTA (Ref. 13) is used to convect the turbulent field downstream over the aircraft. Further discussion regarding the turbulence generated can be found in Reference 8. Presently, the turbulent field is characterized by a mean windspeed of 10.3 m/s (20 kt) and turbulence intensity of 30% (corresponding to the "Severe case" from Ref. 8). The trim values for each aircraft in a 20 kt headwind is shown in Table 3. All vehicles have a similar pitch attitude where the difference is caused by the aircraft having different flat plate drag areas (scales with gross weight). Each aircraft is placed within the same turbulent field and are assumed to be spatially fixed as the turbulence washes over the aircraft. This is done to restrict the aircraft from moving out of the generated flow field.

Table 3. Aircraft Trim at 20 kt

Gross Weight (lb)	50	300	680	1200
Pitch Attitude (deg)	-1.8°	-1.7°	-1.7°	-1.6°
Front Rotor Speed (RPM)	4700	1900	1270	950
Rear Rotor Speed (RPM)	5510	2230	1490	1110
Front Motor Voltage (V)	25.5	63.1	94.6	126.2
Rear Motor Voltage (V)	26.7	70.9	106.4	141.8
Front Motor Current (A)	23.3	57.7	86.5	115.4
Rear Motor Current (A)	29.7	73.1	109.7	146.2

The velocity associated with turbulence is interpolated across each rotor disk at the BET integration points, varying the forces and moments produced by each rotor. This is summarized by Fig. 1, where the axial component of turbulence is represented by $V'_{\hat{z}}$, and the edgewise component is represented by $V'_{\hat{x}}$, where ${}^b[\hat{x},\hat{y},\hat{z}]$ is the blade element reference frame.

The axial component of the turbulence ($V'_{\hat{z}}$) is most critical to the variation of forces and moments produced by the rotor, as $V'_{\hat{z}}$ is about the same order of magnitude as U_P, while the tangential velocity is dominated by the rotor speed ($U_T = V_x \sin\psi + \Omega r >> V'_{\hat{x}}$). Overall, this results in the aerodynamic angle of attack being more sensitive to U'_P than it is to U'_T. Further discussion can be found in Ref. 8.

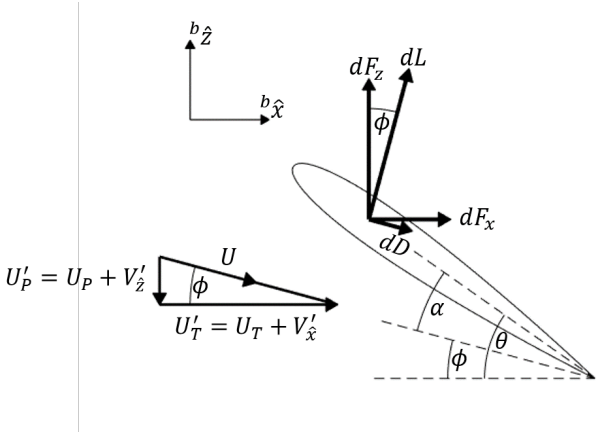

Figure 1. Turbulence Application at Blade Element

Although all four aircraft are within the same turbulent field, each rotor will experience slightly different turbulent velocities at the rotor integration points, as the rotor boom length scales with the vehicle size (a $0.1R$ rotor tip clearance is maintained). As a representative case, the time history for the turbulent velocities at the rotor 1 hub (front-right rotor) of the 1200 lb vehicle is shown in Fig. 2. While the peaks and troughs experienced by the other vehicles will be quantitatively different due to the rotor locations, the stochastic distribution and frequency content of the velocities will be similar. Therefore, Fig. 2 qualitatively represents the turbulence at each rotor of each aircraft.

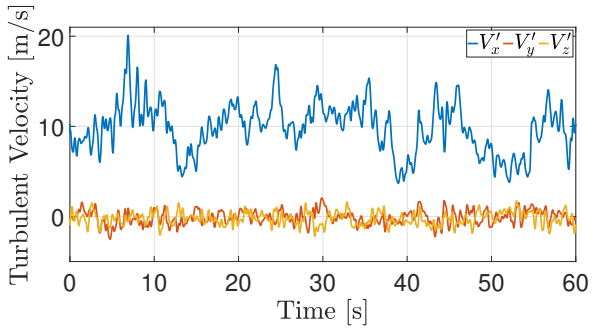

Figure 2. Turbulence at 1200 lb Aircraft Rotor 1 Hub

The mean and standard deviation of the turbulent velocities at the rotor 1 hub of each aircraft is shown in Table 4. In this 60 second window of turbulence all aircraft see mean longitudinal turbulence velocities between 9.7-9.9 m/s (18.9-19.2 kt). This is slightly lower than the prescribed mean windspeed (10.3 m/s or 20 kt) from the turbulence generation. This discrepency is due to the stochastic nature of the turbulent field, where over a long enough timespan, the mean windspeed would converge to the prescribed value.

As previously discussed, the critical component of turbulence is the velocity variation through the rotor disk, V'_z; therefore, the longitudinal and lateral components of turbulence will not be discussed. The frequency content of the axial turbulent

Table 4. Mean and Standard Deviation of Turbulent Velocity at Aircraft Rotor 1 Hub

Gross Weight	V'_x (m/s)		V'_y (m/s)		V'_z (m/s)	
	μ	σ	μ	σ	μ	σ
50 lb	9.73	2.77	-0.05	0.82	-0.44	0.71
300 lb	9.92	2.73	-0.15	0.76	-0.21	0.63
680 lb	9.86	2.82	-0.22	0.76	-0.24	0.69
1200 lb	9.77	2.72	-0.12	0.76	-0.22	0.72

component is shown in Fig. 3, where there is a corner frequency of approximately 1 Hz, followed by a rapid decrease in frequency content. From this, the majority of the energy in the disturbance is in the low frequency range.

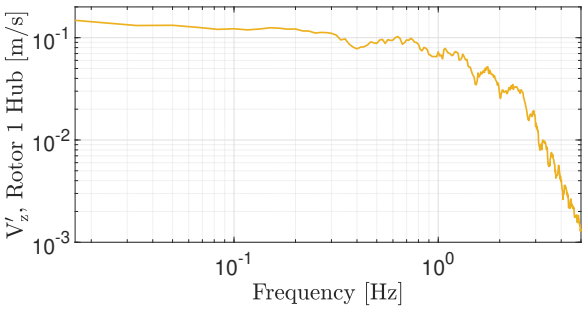

Figure 3. Axial Turbulence Frequency Content at 1200 lb Rotor 1 Hub

Flight Controller

All aircraft utilize explicit-model-following controllers (detailed in Ref. 14) with the architecture shown in Fig. 4. This architecture is characterized by feedforward paths defined by a low order inverse model (based on hovering vehicle), and feedback PID controllers which stabilize the aircraft and reject disturbances. Disturbance inputs in the feedback paths are used for the evaluation of the disturbance rejection specifications (disturbance rejection peak and bandwidth). During simulation the turbulence is directly applied to the plant. Sensors are placed in the feedback paths for the aircraft attitudes, angular rates, and velocities, where the sensors are modeled as well-damped second-order filters with a natural frequency of 100 Hz (Ref. 14). All aircraft feature an outer-loop controller, which tracks disturbances to the aircraft velocities and works to maintain zero groundspeed.

Flight controllers are tuned using CONDUIT® (Ref. 14), a multi-objective control optimization suite which tunes feedback gains to meet a set of HQ specifications (which include ADS-33E-PRF, Ref. 15) while minimizing actuator effort. In previous studies, CONDUIT®has been used to tune controllers for UAM/AAM multicopters (Refs. 4,6,7), using both nominal and Froude-scaled specifications. The present study utilizes similar controllers designed in Ref. 6, where the controllers are tuned to the same specifications and slight modi-

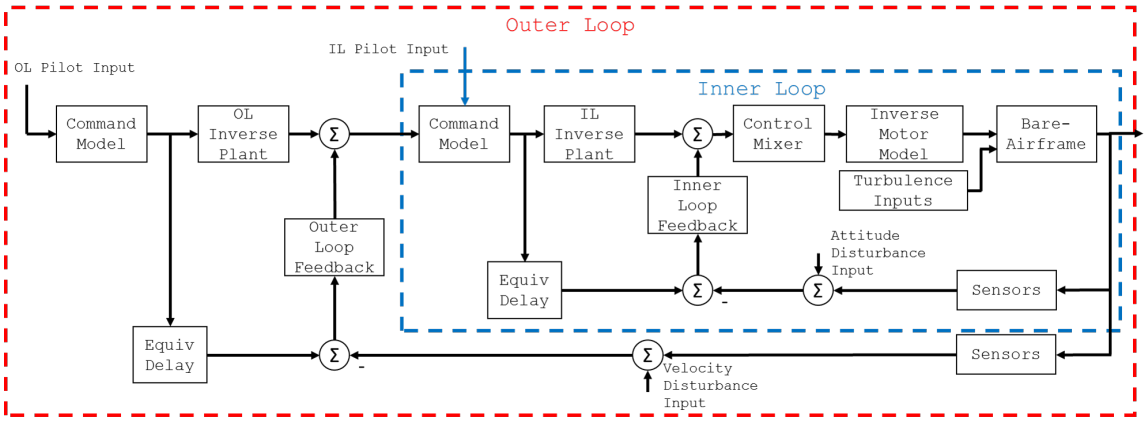

Figure 4. Control Architecture

fications to the gains are made to account for sensors in the feedback paths.

When using the nominal controller all vehicles are held to the same specifications when tuning the flight controller. As the aircraft scale decreases from the nominal 1200 lb aircraft, certain specifications are scaled (using Froude-scaling, Ref. 16) to improve the handling of the smaller aircraft, as they are more agile. The scaling parameter, F, is defined in Eq. 1 and the parameters which are scaled are presented in Table 5.

$$F = \sqrt{\frac{\text{Rotor Radius}}{\text{Reference Rotor Radius}}} \tag{1}$$

Table 5. Froude-Scaling per Dimension

Dimension	Units	Scaling
Length	m	F^2
Time	s	F
Attitude	rad	-
Frequency	rad/s	F^{-1}
Velocity	m/s	F

For turbulence rejection, the key specifications are disturbance rejection peak (DRP) and bandwidth (DRB), where the DRB scales with the aircraft size (DRB scales with $1/F$) and DRP is unscaled. The effect that scaling has on the DRB and DRP is shown in Fig. 5, which represents the longitudinal velocity disturbance transfer function for the 50 lb vehicle (where the largest scaling occurs). Scaling the controller moves the DRB from 0.69 rad/s to 1.55 rad/s (0.11 Hz to 0.25 Hz), and doesn't substantially change the DRP. The change in DRB and DRP for all aircraft is summarized in Table 6.

Scaling is most effective on the 50 lb aircraft, where the DRB increases substantially, and the DRP slightly decreases. A decrease in the DRP will have the effect of reducing the amplitude of the disturbances which are not attenuated by the controller. However, this is not a dominant effect after scaling; as a 0.25 dB decrease is a 2.3% reduction in magnitude.

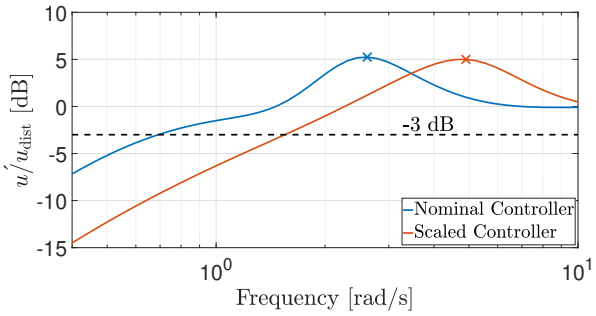

Figure 5. 50 lb Aircraft Longitudinal Disturbance

Similar changes in DRB and DRP are observed in the lateral and heave axes and are not presented.

Table 6. Longitudinal Velocity Disturbance Rejection Bandwidth and Peak

Aircraft	Nominal	Scaled
	DRB (rad/s)	
50 lb	0.69	1.55
300 lb	0.67	0.88
680 lb	0.68	0.70
1200 lb	0.68	–
	DRP (dB)	
50 lb	5.02	4.74
300 lb	4.89	4.98
680 lb	4.94	4.92
1200 lb	4.99	–

RESULTS

Inner-Loop Response

In the presence of turbulence, the aircraft will deviate from their trim condition due to the variations in forces and moments produced by each rotor. The pitch response of all aircraft within the turbulent field is qualitatively similar, and is

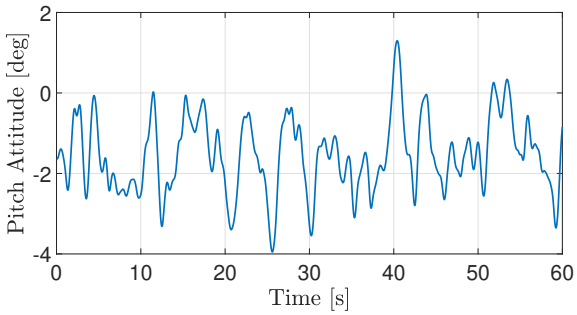

Figure 6. 1200 lb Aircraft Pitch Response

represented by the 1200 lb aircraft (see Fig. 6). The response is characterized by oscillation about the trim pitch attitude ($-1.6°$, Table 3), while the other axes oscillate about zero.

The overall attitude response for all aircraft using the nominal controller is summarized in Fig. 7, where the flight controllers for all aircraft are held to the same specifications. The dashed line in each box plot represents the mean attitude for each aircraft, with the upper and lower limits of each box representing 75th and 25th percentiles of the signal, respectively. The error bars represent the peak-to-peak values of the signal and show the minimum and maximum as the lower and upper limits, respectively.

In roll, all aircraft are centered about a mean roll attitude of zero degrees, with the 50 lb aircraft seeing the largest peak-to-peak attitude at 7.7°. As the aircraft increase in size, the peak-to-peak attitude decreases (seen as reduced error bars). The largest aircraft (1200 lb) has a peak-to-peak pitch response of 2.9°. The same trend is seen in pitch, where the smallest aircraft has the largest peak-to-peak response (9.2°) and the largest vehicle has the lowest peak-to-peak response (5.2°).

However, in yaw the largest vehicles have the highest peak-to-peak disturbance ($\sim$1.3° for the 680 and 1200 lb aircraft); this is due to the vehicle inertia scaling faster than the motor torque. Yaw also has the lowest peak-to-peak disturbance compared to roll and pitch. Which is due to yaw being actuated by motor torque, rather than rotor thrust; and motor torque is not affected by turbulence (aerodynamic torque on the rotor is).

As the vehicles decrease in size, the attitude disturbance increases due to the decrease in inertia (as all aircraft have similar DRB and DRP, Table 6). The stability and control derivatives for each aircraft are shown in Table 7. The roll and pitch stability derivatives increase with the vehicle scale; therefore, as the vehicle scale increases, disturbances in pitch and roll are more damped by the vehicle inertia.

Table 7. Pitch and Roll Stability and Control Derivatives

Aircraft	L_p	M_q	$L_{\delta\Omega_{1s}}$	$M_{\delta\Omega_{1c}}$
50 lb	-0.33	-0.28	-0.07	-0.06
300 lb	-0.59	-0.49	-0.13	-0.11
680 lb	-0.74	-0.63	-0.16	-0.14
1200 lb	-0.87	-0.74	-0.19	-0.16

Implementing scaled controllers on the smaller aircraft results in a reduction of the peak-to-peak disturbances, which is shown in Fig. 8 with the peak-to-peak values tabulated in Table 8. When scaled controllers are used, the peak-to-peak disturbance in each axis is similar for all aircraft. While using the nominal controllers the peak-to-peak pitch response varied from 9.2° for the 50 lb aircraft, down to 5.2° for the 1200 lb aircraft (4° difference). After scaling, the peak-to-peak pitch response is between 4.8° and 5.2° (only a 0.4° difference). Similar reduction in peak-to-peak is seen in the roll attitude; when using the nominal controller there was a 4.8° peak-to-peak difference across the aircraft, after scaling the difference is 0.5°.

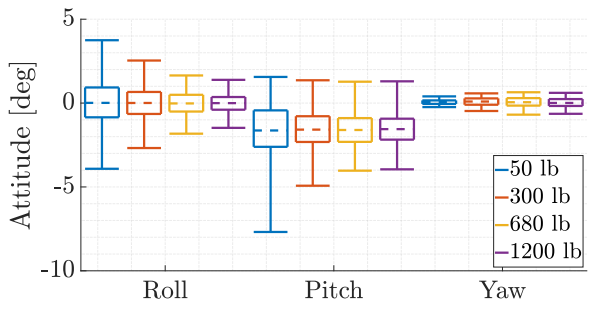

Figure 7. Aircraft Attitude Response Nominal Controller

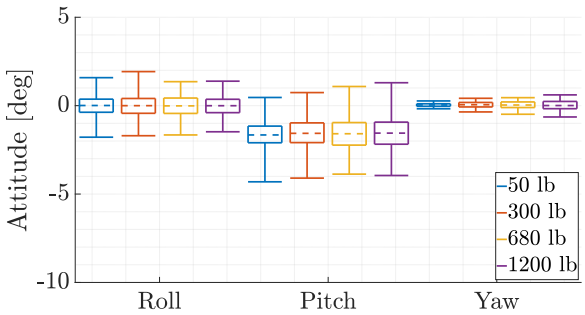

Figure 8. Aircraft Attitude Response Scaled Controller

Table 8. Peak-to-Peak Attitude Disturbance

Aircraft	ϕ Nominal	ϕ Scaled	θ Nominal	θ Scaled	ψ Nominal	ψ Scaled
50 lb	7.66°	3.37°	9.24°	4.77°	0.64°	0.44°
300 lb	5.22°	3.63°	6.29°	4.84°	1.05°	0.77°
680 lb	3.47°	3.01°	5.30°	4.96°	1.34°	0.94°
1200 lb	2.86°	–	5.25°	–	1.25°	–

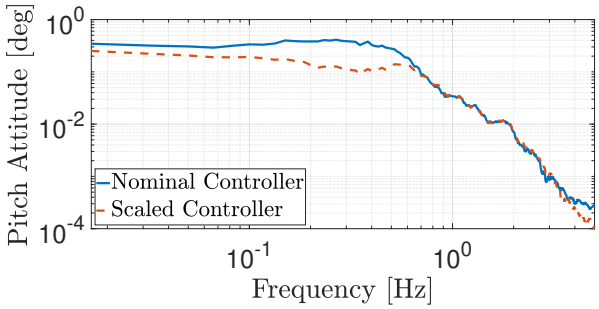

Figure 9. Pitch Attitude Frequency Content 50 lb Aircraft

Comparing the frequency content of the pitch attitude for the nominal and scaled 50 lb aircraft, shown in Fig. 9, shows that at low frequencies (below 0.6 Hz) the scaled controller reduces the frequency content in the aircraft pitch attitude. This is due to the DRB increasing for the scaled controller. At frequencies above 0.6 Hz, the frequency content decreases for both controllers. This is due to the aircraft inertia filtering out the disturbance, as well as the turbulence content decreasing at higher frequencies.

Outer-Loop Response

The controller implemented on each aircraft uses a translational rate command (TRC) response type in the longitudinal, lateral, and heave axes, with the feedback path rejecting disturbances to the aircraft groundspeed. Figure 10 shows the body velocity response when using the nominal controller where all aircraft have a mean response of 0 m/s, while the smallest aircraft sees the largest peak-to-peak change in velocity at 1.11 m/s, 0.77 m/s, and 0.34 m/s in u, v, and w, respectively. Similar to the inner-loop responses, as the vehicle scale increases the peak-to-peak disturbance decreases due to the increasing vehicle inertia.

Scaling the controllers decreases the peak-to-peak body velocities caused by turbulence (See Fig. 11), and the comparison between nominal and scaled controller is tabulated in Table 9. The scaled controller drastically improves the response of the smallest aircraft, bringing the longitudinal velocity response of the 50 lb aircraft from 1.11 m/s to 0.34 m/s. Similar improvement is seen for the 300 lb aircraft. However, the 680 lb aircraft does not see a substantial reduction in the peak-to-peak response, as this aircraft is not scaled as aggressively. In the inner-loop, scaling the controllers caused all four aircraft to have similar peak-to-peak responses in pitch and roll attitude which is not the case for the outer-loop, where the smaller aircraft outperform the larger ones (seen as smallest aircraft having the smallest peak-to-peak values, see Fig. 11).

The nominal aircraft all have similar heave and sway responses, with peak-to-peak heave rates between 0.32-0.39 m/s and a mean of 0 m/s. Scaling the controllers improves the response, reducing the peak-to-peak heave rates to be between 0.25-0.32 m/s.

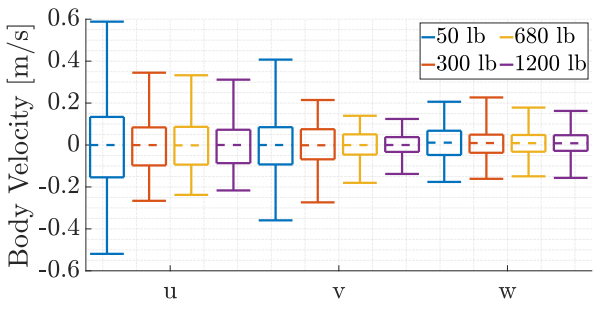

Figure 10. Velocity Response Nominal Controller

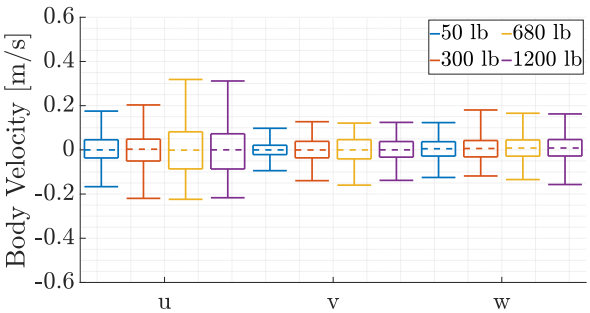

Figure 11. Velocity Response Scaled Controller

Table 9. Peak-to-Peak Velocity Disturbance

Aircraft	u Nominal	u Scaled	v Nominal	v Scaled	w Nominal	w Scaled
50 lb	1.11 m/s	0.34 m/s	0.77 m/s	0.19 m/s	0.38 m/s	0.25 m/s
300 lb	0.61 m/s	0.42 m/s	0.49 m/s	0.27 m/s	0.39 m/s	0.30 m/s
680 lb	0.57 m/s	0.54 m/s	0.32 m/s	0.28 m/s	0.33 m/s	0.30 m/s
1200 lb	0.53 m/s	–	0.26 m/s	–	0.32 m/s	–

Rotor Speed

The aircraft modeled in this study feature fixed-pitch rotors; therefore, the rotors must constantly change speed to produce the forces and moments necessary to reject the disturbance due to turbulence. As before, the front and rear rotor speed response will qualitatively be represented by the 1200 lb vehicle using the nominal controller, shown in Fig. 12. The response is characterized by the front and rear rotors oscillating about a mean rotor speed (980 RPM for front, 1090 RPM for rear). These mean rotor speeds differ from the trim values (Table 3); as the mean turbulence velocity is less than the trim velocity, resulting in less of a required differential rotor speed from the rotors.

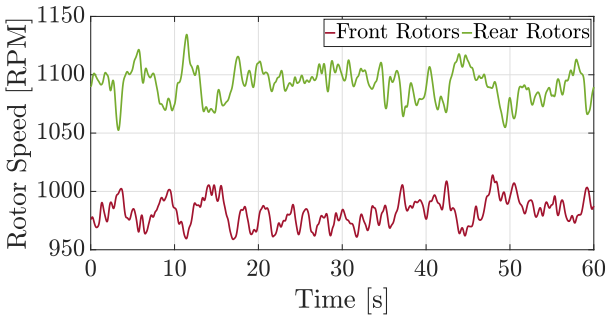

Figure 12. Rotor Speed Response of 1200 lb Aircraft

As the vehicle scale decreases, the rotors become smaller and must increase in speed (to maintain the same tip speed, Table 2). Therefore, the rotor speed responses for the smaller aircraft would be characterized by a larger mean rotor speed, and larger peak-to-peak variations in speed (not shown).

Motor Current

The variation of rotor speed described in the preceding section will require rapid actuation of the electric motors, delivering torque to the rotors (via current fluctuations). The overall current response for the 1200 lb aircraft is shown in Fig. 13; where the response is characterized by the rear rotors having the largest mean current (due to the rear rotors spinning faster, Fig. 12). The rear rotors also have a larger peak-to-peak variation in current (the 25th and 75th percentiles are also wider), indicating they are more active than the front rotors.

An important parameter for vehicle design is the peak motor torque, as it determines the size of the electric motors installed

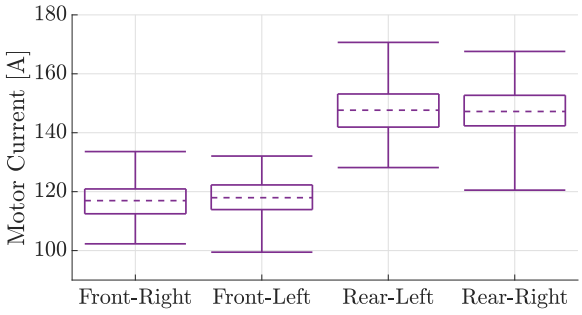

Figure 13. Current Response of 1200 lb Aircraft

on the aircraft. The peak motor torque is linearly related to the motor current, as $\tau = iK_t$ (K_t is the motor torque constant). For the 1200 lb aircraft, motor 3 (rear-left motor) experiences the highest peak torque out of the four rotors. This is true for all aircraft in this study and is due to the specific turbulence used (a different turbulence field may cause the rear-right motors to have the highest peak torque).

The current margin represents the additional current (above hover current) that is required to reject turbulence or perform a maneuver; where the current margin is related to the peak current through Eq. 2,

$$i_{\text{peak}} = i_{\text{trim}}(100\% + \text{Current Margin}). \tag{2}$$

The current margin for each aircraft using the nominal controllers is shown in Fig, 14, where the four vehicles require similar margin to reject turbulence (between 9%-12%). Overall, this is much lower than the current margin required to perform maneuvers; which was previously found to be about 25% (Refs. 6,7). Using the scaled controllers (see Fig. 15) the required current margin increases for the scaled aircraft, causing the current margin to be between 11%-12.5%. The current margin for each aircraft is tabulated in Table 10, showing the change from the nominal to scaled controller. The 50 lb vehicle sees the largest change in current margin, increasing from 10.5% to 12.5%. The 300 lb and 680 lb aircraft see similar increases, resulting in a scaled current margin of 11.1% and 11.2%, respectively. Even after scaling, the current margin remains well below the margin required for maneuver; showing that turbulence rejection is not the limiting factor for motor sizing.

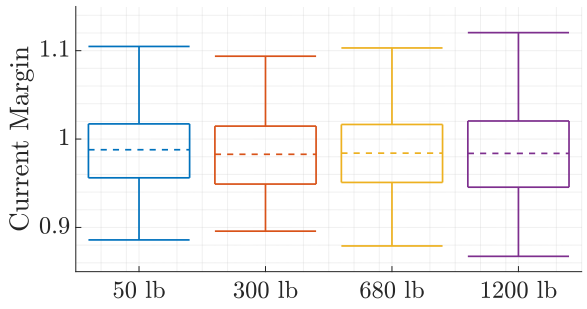

Figure 14. Current Margin Nominal Controllers

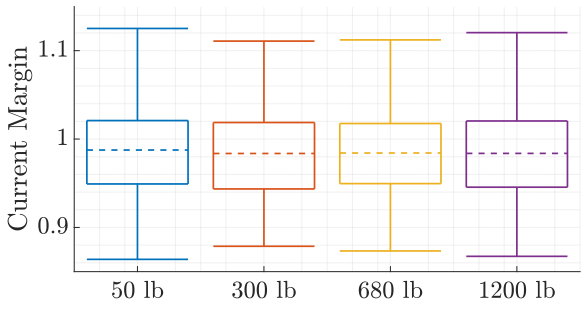

Figure 15. Current Margin Scaled Controllers

Table 10. Required Current Margins

Aircraft	Hover Current	Nominal Current Margin	Scaled Current Margin
50 lb	30.4 A	10.5%	12.5%
300 lb	75.0 A	9.37%	11.1%
680 lb	112 A	10.3%	11.2%
1200 lb	150 A	12.0%	12.0%

While the peak current does not substantially increase when the flight controllers are scaled (meaning the motors do not need to increase in weight), the actuator activity does increase; which is shown via the RMS motor current where the RMS current is calculated from Eq. 3,

$$i_{\text{RMS}} = \sqrt{\frac{1}{T}\int_0^T (i(t) - i_{\text{mean}})^2 \, dt}. \tag{3}$$

The RMS current for motor 3 (rear-left rotor, highest trim current) is tabulated in Table 11, showing that scaling the controllers significantly increases the RMS current, by as much as 23.6% for the 50 lb aircraft. Scaling most significantly increases the RMS current for the smallest aircraft, where the percent change decreases as the aircraft gets larger (controller is scaled less aggressively for larger aircraft).

Table 11. Motor 3 RMS Current

Aircraft	Nominal RMS	Scaled RMS	Percent Change
50 lb	1.34 A	1.65 A	23.6%
300 lb	3.35 A	3.86 A	15.3%
680 lb	5.46 A	5.72 A	5.80%
1200 lb	8.19 A	–	–

The percent change in RMS current across all rotors is summarized by Table 12. Which shows that the smallest aircraft have the largest increase in RMS current, an expected result due to the Froude-scaling. Overall, similar trends are seen across all aircraft, where the rear rotors have a larger increase in RMS current (compared to the front rotors).

Table 12. Percent Change in RMS Current Following Scaling

Aircraft	Motor 1	Motor 2	Motor 3	Motor 4
50 lb	17.0%	20.9%	23.6%	17.8%
300 lb	11.2%	11.7%	15.3%	13.8%
680 lb	2.1%	2.5%	5.8%	4.2%

CONCLUSIONS

Disturbance rejection capabilities of different sized quadcopters (50-1200 lb) is evaluated by analyzing the aircraft rigid body response and required motor current under atmospheric turbulence at 20 kt and 30% TI. Under nominal conditions, the flight controllers for each aircraft were tuned to meet baseline HQ specifications. The flight controllers for the small aircraft were Froude-scaled to utilize the increased agility of the smaller aircraft, and improve disturbance rejection capabilities. The following conclusions are made:

- Using nominal controllers, the smaller aircraft experience larger disturbances in the presence of atmospheric turbulence due to lower inertia. The 50 lb aircraft has a 9.2° peak-to-peak pitch response, compared to 5.2° for the 1200 lb aircraft.
- Froude-scaling the flight controller specifications improves the disturbance rejection capabilities of the smaller aircraft. This results in the inner-loop responses having practically the same peak-to-peak disturbance across all aircraft. Scaling brought the difference in peak-to-peak pitch response across the four aircraft from 4° to 0.4°. In roll, scaling reduced the difference in peak-to-peak attitude from 4.8° to 0.5°.
- Scaling the flight controllers comes at the cost of increasing actuator activity, increasing the current RMS of the most active motor by 24%, 16%, and 8% for the 50 lb, 300 lb, and 680 lb aircraft, respectively.
- The peak current (important for motor sizing) does not substantially increase after scaling the controllers. The current margin increases from 10.5% to 12.5% for the 50 lb aircraft. The current margin required to reject turbulence does not limit the sizing of the motors, as it is less than what is required for maneuver.

Author contact:
Matthew Bahr: bahrm2@rpi.edu
Etana Ferede: ferede@rpi.edu
Farhan Gandhi: gandhf@rpi.edu

REFERENCES

1. Thedin, R., Murman, S. M., Horn, J., and Schmitz, S., "Effects of Atmospheric Turbulence Unsteadiness on Ship Airwakes and Helicopter Dynamics," *Journal of Aircraft*, Vol. 57, (3), 2020, pp. 534–546. DOI: 10.2514/1.C035643

2. Oruc, I., Horn, J. F., Polsky, S., Shipman, J., and Erwin, J., "Coupled Flight Dynamics and CFD Simulations of the Helicopter / Ship Dynamic Interface," American Helicopter Society 71st Annual Forum, Virginia Beach, VA, May 2015.

3. Silva, C., Johnson, W., Antcliff, K. R., and Patterson, M. D., "VTOL Urban Mobility Concept Vehicles for Technology Development," Aviation Technology, Integration, and Operations Conference, Atlanta, GA, June 2018. DOI: https://doi.org/10.2514/6.2018-3847

4. Malpica, C., and Withrow-Maser, S., "Handling Qualities Analysis of Blade Pitch and Rotor Speed Controlled eVTOL Quadrotor Concepts for Urban Air Mobility," VFS International Powered Lift Conference, San Jose, CA, January 2020.

5. Withrow-Maser, S., Malpica, C., and Nagami, K., "Multirotor Configuration Trades Informed by Handling Qualities for Urban Air Mobility Application," VFS 76th Annual Forum & Technology Display, Virtual, October 6–8, 2020.

6. Walter, A., McKay, M., Niemiec, R., and Gandhi, F., "Hover Handling Qualities of Fixed-Pitch, Variable-RPM Quadcopters with Increasing Rotor Diameter," Vertical Flight Society 76th Annual Forum, Virtual, October 6–8, 2020.

7. Bahr, M., McKay, M., Niemiec, R., and Gandhi, F., "Handling Qualities of Fixed-pitch, Variable-speed Multicopters for Urban Air Mobility," *The Aeronautical Journal*, 2021, pp. 1–21. DOI: 10.1017/aer.2021.114

8. Bahr, M., Hebbar, U., Ferede, E., and Gandhi, F., "Multi-rotor eVTOL Flight Simulation and Assessment Under Atmospheric Turbulence," Vertical Flight Society 77th Annual Forum, Virtual, May 10–14, 2021.

9. Niemiec, R., and Gandhi, F., "Development and Validation of the Rensselaer Multicopter Analysis Code (RMAC): A Physics-Based Comprehensive Modeling Tool," Vertical Flight Society 75th Annual Forum, Philadelphia, PA, May 2019.

10. Peters, D., Boyd, D., and He, C. J., "Finite-State Induced-Flow Model for Rotors in Hover and Forward Flight," *Journal of the American Helicopter Society*, Vol. 34, (4), 1989, pp. 5–17.

11. Singh, R., Hrishikeshavan, V., and Sirohi, J., "Common Research Configuration for Collaborative Advancement of Scalable VTOL UAS Technologies," VFS 75 Annual Forum & Technology Display, Philadelphia, PA, May 13–16, 2019.

12. Kelley, N., and Jonkman, B., "Overview of the TurbSim Stochastic Inflow Turbulence Simulator," Technical Report National Renewable Energy Lab (NREL), Golden, CO, 2006.

13. Tran, S., and Sahni, O., "Finite element-based large eddy simulation using a combination of the variational multiscale method and the dynamic Smagorinsky model," *Journal of Turbulence*, Vol. 18, (5), 2017, pp. 391–417. DOI: 10.1080/14685248.2017.1280607

14. Tischler, M., Berger, T., Ivler, C., Mohammadreza, M. H., Cheung, K. K., and Soong, J. Y., "Practical Methods for Aircraft and Rotorcraft Flight Control Design: An Optimization-Based Approach," AIAA Education Series, Reston, VA, 2017.

15. "ADS-33E-PRF, Aeronautical Design Standard, Performance Specification, Handling Qualities Requirements for Military Rotorcraft," Technical Report ADS-33E-PRF, March 2000.

16. Alvarenga, J., Vitzilaios, N. I., Rutherford, M. J., and Valavanis, K. P., "Scaled Control Performance Benchmarks and Maneuvers for Small-Scale Unmanned Helicopters," IEEE 54th Annual Conference on Decision and Control (CDC), Osaka, Japan, December 15–18, 2015.